Chapter 1
Leader-follower synchronisation for a class of underactuated systems

Dennis J.W. Belleter and Kristin Y. Pettersen *

Abstract In this work leader-follower synchronization is considered for underactuated followers in an inhomogeneous multi-agent system. The goal is to synchronise the motion of a leader and an underactuated follower. Measurements of the leader's position, velocity, acceleration, and jerk are available, while the dynamics of the leader is unknown. The leader velocities are used as input for a constant bearing guidance algorithm to assure that the follower synchronises its motion to the leader. It is also shown that the proposed leader-follower scheme can be applied to multi-agent systems that are subjected to unknown environmental disturbances. Furthermore, the trajectory of the leader does not need to be known. The closed-loop dynamics are analysed and it is shown that under certain conditions all solutions remain bounded and the synchronisation error kinematics are shown to be integral input-to-state stable with respect to changes in the unactuated sway velocity. For straight-line motions, i.e. where the desired yaw rate and sway velocity go to zero, synchronisation is achieved. Simulation results are presented to validate the proposed control strategy.

1.1 Introduction

This work considers leader-follower synchronisation for inhomogeneous multi-agent systems with underactuated agents. In particular we consider synchronisation of underactuated marine vessels on straight-line trajectories and curved paths. Leader-follower synchronisation also has several applications concerning both au-

Dennis J.W. Belleter and Kristin Y. Pettersen
Centre for Autonomous Marine Operations and Systems (AMOS) and the Department of Engineering Cybernetics, Norwegian University of Science and Technology, NO7491 Trondheim, Norway, e-mail: dennis.belleter,kristin.y.pettersen@itk.ntnu.no

* This work was partly supported by the Research Council of Norway through its Centres of Excellence funding scheme, project No. 223254 AMOS.

tonomous and nonautonomous vehicles. Leader-follower synchronisation has for instance been applied to underway replenishment operations, robot manipulator master-slave synchronisation, and formation control tasks.

In the marine systems literature work leader-follower synchronisation has played an important part in research on underway replenishment of ships, see for instance [15], [19], and [24]. For these operations the supply-ship is usually responsible for synchronising its motion with the ship it is supplying. In [19] the case of a fully actuated follower that synchronises its output with a leader with unknown dynamics is investigated. An observer-controller scheme is utilised to achieve synchronisation where the observers are used to estimate the unknown velocities of the leader and follower. The observer-controller scheme utilised in [19] is based on theory for master-slave synchronisation of robotic manipulators investigated in [21]. In [24] the focus is on interaction forces between two vessels during underway replenishment operations. For control purposes the constant bearing guidance algorithm from [6] is used to synchronise the ships along a straight-line path. The vessels are underactuated, but no analysis of the underactuated internal dynamics are given. In [15] underway replenishment between fully actuated vessels is investigated and adaptive backstepping controllers are designed to reject exogenous disturbances.

Leader-follower synchronisation is also widely applied for other coordinated control applications. Applications include master-slave synchronisation of robot manipulators in [21], leader-follower synchronisation for control of mobile robots in [2, 11, 23, 10], and for formation control of marine vessels in [7]. For these applications the models are either fully actuated or formulated only at the kinematic level. However, most commercial systems are underactuated or become underactuated at higher speed, e.g., vessels with a tunnel thruster to apply a sideways force are fully actuated for low speeds but the tunnel thruster becomes inefficient at cruising speed, see [9] and the references therein. Also cars and most mobile robots are underactuated (nonholonomic) systems. Furthermore many marine vehicles and autonomous aerial vehicles are second-order holonomic systems with internal dynamics that are not asymptotically stable, i.e., are non-minimum phase systems. A formation control strategy that can be applied to underactuated multi-agent systems is considered in [16] where hybrid control techniques are used. The approach is based on consensus rather than leader-follower synchronisation and does not take into account disturbance rejection. In [22] formation control of underactuated vessels under the influence of constant disturbances is considered using neural network adaptive dynamic surface control to track pre-defined paths.

In [4] formation control of underactuated systems is considered, and straight-line path following in formation is achieved for underactuated marine vessels under the influence of constant ocean currents. Straight-line target tracking for underactuated unmanned surface vessels is investigated in [8]. In [8] constant bearing guidance is used to track a target moving in a straight line, experimental results are presented but closed loop stability is not proven.

The case considered in this work is leader-follower synchronisation for an underactuated follower in an inhomogeneous multi-agent system. The multi-agent system can thus consist of a leader with arbitrary dynamics as long as it moves in the

same space as the follower(s). The follower can be any type of vehicle described by the nonlinear manoeuvring model that is introduced in the next section. For formation control purposes each follower can again be the leader of other followers, or all followers can have the same leader. Examples of possible configurations are autonomous surface vessels (ASV) following an autonomous underwater vehicle (AUV) as communication nodes during AUV search and survey operations, or a fleet of ASVs manoeuvring by following a leader. Since we consider an underactuated system we need to take into account the full dynamic model in the control design and analysis. In particular, since the system is underactuated it is not possible to consider a purely kinematic model since then the internal sway dynamics cannot be analysed. Moreover for the case considered here it is not possible to perform feedback linearisation of the full dynamics. The leader dynamics and the leader trajectories are assumed to be unknown. The leader is free to move as it wants independently of the follower, but the follower has access to measurements of the leader's position and velocity in the inertial frame for use in the guidance law. If the follower uses controllers with acceleration feedforward the leader's acceleration and jerk also need to be measured. This includes cases where there is communication between the leader and follower, but also when the follower reads AIS measurements of the leader [18].

It should be noted that the leader-follower synchronisation scheme in this work has its dual problem in trajectory tracking. Hence, the input signal of the leader could easily be replaced by a virtual leader. This is true for most, if not all, leader-follower type synchronisation schemes since the leader can always be represented as a virtual vehicle with known trajectory and properties. However, when performing trajectory tracking in most cases it is preferable to use information about the dynamics of the vehicle since then perfect tracking can be achieved for all types of motions. When the leader dynamics and desired trajectory are not known a priori the followers' internal dynamics might be perturbed by the chosen leader motion. Moreover when the strategy is applied in a chained form, i.e., followers become leaders to other vehicles, the duality is lost. The stability properties derived in this work will still hold with respect to each leader. However, string stability is not considered in this work and should be investigated to analyse the error propagation along the chain of vehicles.

Preliminary results for this problem have been presented in [5], where the followers' yaw rate was used as a parameter to limit the motion of the follower to reduce the synchronisation error. However, in this work the effect of the internal dynamics was not considered in the analysis of the guidance. In this chapter we generalize the results of [5] by analysing the complete closed-loop system including the fully actuated closed-loop dynamics, the underactuated sway dynamics in addition to the synchronisation error kinematics. We discuss the conditions to achieve synchronisation and the physical meaning of these conditions. In particular, we show that the synchronisation error kinematics become integral input-to-state stable (iISS) with respect to changes in the velocity when coupled with the underactuated dynamics, i.e. perfect synchronisation is not possible on trajectories that excite the underactuated dynamics. Moreover, we also prove that the constant bearing guidance gives

uniformly semiglobally exponentially stable (USGES) synchronisation error kinematics, rather then simply uniformly globally asymptotically stable (UGAS) and uniformly locally exponentially stable (ULES) as proved in previous work.

The work is organised as follows. In Section 1.2 the dynamic model for the follower and the constant bearing guidance algorithm are introduced. The closed-loop behaviour is investigated in Section 1.3. Section 1.4 presents simulations considering different scenarios. Finally Section 1.5 gives the conclusions of the work.

1.2 The Follower

This section presents the model for the follower and the guidance law for the follower that is used to synchronise its motion to that of the leader. The leader-follower synchronisation scheme is developed for a class of systems described by a 3-DOF manoeuvring model. This class of systems includes underactuated autonomous surface vessels (ASV) and autonomous underwater vehicles (AUV) moving in the horizontal plane. However, it should be noted that the leader-follower scheme and analysis can be extended to different classes of systems with similar properties such as unmanned aerial vehicles by considering the appropriate dynamic model, control/guidance scheme, and appropriate disturbances.

1.2.1 The Vessel Model

We consider an ASV or AUV moving in the horizontal plane. The motion of the vessel is described by the position and orientation of the vessel w.r.t. the earth-fixed reference frame, i.e., $\eta \triangleq [x, y, \psi]^T$. For marine craft the earth-fixed north-east-down (NED) frame is usually used as inertial frame [12]. The vector of linear and angular velocities is given in the body-fixed reference frame by $\nu \triangleq [u, v, r]^T$, containing the surge velocity u, sway velocity v, and yaw rate r. The vessel is disturbed by an ocean current expressed in the inertial frame n, i.e., the earth-fixed frame. The current is denoted by V_c and satisfies the following assumption.

Assumption 1. The ocean current is assumed to be constant and irrotational w.r.t. n, i.e., $V_c \triangleq [V_x, V_y, 0]^T$. Furthermore, it is bounded by $V_{\max} > 0$ such that $\|V_c\| = \sqrt{V_x^2 + V_y^2} \leq V_{\max}$.

The ocean current velocity is expressed in the body-fixed frame b and is denoted by $\nu_c \triangleq [u_c, v_c, 0]^T$. It can be obtained by $\nu_c = R(\psi)^T V_c$ where $R(\psi)$ is the rotation matrix from the body to inertial frame defined as

$$R(\psi) \triangleq \begin{bmatrix} \cos(\psi) & -\sin(\psi) & 0 \\ \sin(\psi) & \cos(\psi) & 0 \\ 0 & 0 & 1 \end{bmatrix}. \tag{1.1}$$

The vessel model is expressed in terms of the relative velocity defined as $\nu_r \triangleq \nu - \nu_c = [u_r, v_r, r]^T$ expressed in b. Since the ocean current is constant and irrotational the vessel can be described by the 3-DOF manoeuvring model [12]

$$\dot{\eta} = R(\psi)\nu_r + V_c, \tag{1.2a}$$
$$M\dot{\nu}_r + C(\nu_r)\nu_r + D\nu_r = Bf. \tag{1.2b}$$

The vector $f \triangleq [T_u, T_r]^T$ is the control input vector, containing the surge thrust T_u and the rudder angle T_r. The matrix $M = M^T > 0$ is the system inertia matrix including added mass, C is the Coriolis and centripetal matrix, $D > 0$ is the hydrodynamic damping matrix, and B is the actuator configuration matrix.

Remark 1. By expressing the model in relative velocities the environmental disturbances can be incorporated in the model more easily and controlled more straightforwardly.

Assumption 2. We assume port-starboard symmetry.

Remark 2. Assumption 2 is to the authors' best knowledge satisfied for all commercially available surface and underwater vessels.

The matrices M, D, and B are constant and are defined as

$$M \triangleq \begin{bmatrix} m_{11} & 0 & 0 \\ 0 & m_{22} & m_{23} \\ 0 & m_{23} & m_{33} \end{bmatrix}, D \triangleq \begin{bmatrix} d_{11} & 0 & 0 \\ 0 & d_{22} & d_{23} \\ 0 & d_{23} & d_{33} \end{bmatrix}, B \triangleq \begin{bmatrix} b_{11} & 0 \\ 0 & b_{22} \\ 0 & b_{32} \end{bmatrix}.$$

The non-constant matrix $C(\nu_r)$ can be derived from M (See [12]).

Assumption 3. It is assumed the position of the body-fixed frame is chosen such that $M^{-1}Bf = [\tau_u, 0, \tau_r]^T$.

Remark 3. This is possible as long as the center of mass is located along the centreline of the vessel. Coordinate transformations for this translation can be found in [14].

The model can be written in component form as

$$\dot{x} = u_r \cos(\psi) - v_r \sin(\psi) + V_x, \tag{1.3a}$$
$$\dot{y} = u_r \sin(\psi) + v_r \cos(\psi) + V_y, \tag{1.3b}$$
$$\dot{\psi} = r, \tag{1.3c}$$
$$\dot{u}_r = F_{u_r}(v_r, r) + \tau_u, \tag{1.3d}$$
$$\dot{v}_r = X(u_r)r + Y(u_r)v_r, \tag{1.3e}$$
$$\dot{r} = F_r(u_r, v_r, r) + \tau_r, \tag{1.3f}$$

which is clearly underactuated in sway. Therefore, tracking has to be achieved by a suitable velocity and heading assignment that takes into account the underactuation.

For this purpose constant bearing guidance is used. The definitions of F_{u_r}, $X(u_r)$, $Y(u_r)$, and F_r are given by

$$F_{u_r} \triangleq \frac{1}{m_{11}}(m_{22}v_r + m_{23}r)r - \frac{d_{11}}{m_{11}}u_r, \tag{1.4}$$

$$X(u_r) \triangleq \frac{m_{23}^2 - m_{11}m_{33}}{m_{22}m_{33} - m_{23}^2}u_r + \frac{d_{33}m_{23} - d_{23}m_{33}}{m_{22}m_{33} - m_{23}^2}, \tag{1.5}$$

$$Y(u_r) \triangleq \frac{(m_{22} - m_{11})m_{23}}{m_{22}m_{33} - m_{23}^2}u_r - \frac{d_{22}m_{33} - d_{32}m_{23}}{m_{22}m_{33} - m_{23}^2}, \tag{1.6}$$

$$\begin{aligned} F_r(u_r, v_r, r) \triangleq & \frac{m_{23}d_{22} - m_{22}(d_{32} + (m_{22} - m_{11})u_r)}{m_{22}m_{33} - m_{23}^2}v_r \\ & + \frac{m_{23}(d_{23} + m_{11}u_r) - m_{22}(d_{33} + m_{23}u_r)}{m_{22}m_{33} - m_{23}^2}r. \end{aligned} \tag{1.7}$$

Note that $X(u_r)$ and $Y(u_r)$ are bounded for bounded arguments and $Y(u_r)$ satisfies the following assumption.

Assumption 4. It is assumed that $Y(u_r)$ satisfies

$$Y(u_r) \leq -Y^{\min} < 0, \forall u_r \in [-V_{\max}, U_{\max}].$$

with $U_{\max}$ the maximal surge speed of the follower.

Remark 4. This assumption is satisfied for commercial vessels by design, since $Y(u_r) \geq 0$ would imply an undamped or nominally unstable vessel in sway direction.

1.2.2 Constant Bearing Guidance

This subsection briefly describes constant bearing guidance (CB) as presented in [12] and [6]. CB guidance assigns a desired velocity based on two different components expressed in the earth-fixed frame. The first component is the velocity of the leader $v_l^n = [\dot{x}_l, \dot{y}_l]^T$ which needs to be matched. The second component is the follower-leader approach velocity v_a^n which is proportional, but upper-bounded by a maximum, to the relative position in the earth-fixed frame between the follower and the leader $\tilde{p}^n = [\tilde{x}^n, \tilde{y}^n]^T$ and is aligned along the line-of-sight (LOS) vector. The superscript n denotes that the variable is expressed in the earth-fixed frame. An illustration of the constant bearing guidance can be seen in Fig. 1.1. The desired velocity assignment for constant bearing guidance is given by

$$v_d^n = v_l^n + v_a^n, \tag{1.8}$$

$$v_a^n = -\kappa \frac{\tilde{p}^n}{\|\tilde{p}^n\|}, \tag{1.9}$$

with v_l^n the leader velocity, v_a^n the approach velocity, and

$$\tilde{p}^n \triangleq p^n - p_l^n, \tag{1.10}$$

is the LOS vector between the follower and the leader, where $\|\tilde{p}^n\| \geq 0$ is the euclidean length of this vector and

$$\kappa = U_a^{\max} \frac{\|\tilde{p}^n\|}{\sqrt{(\tilde{p}^n)^T \tilde{p}^n + \Delta_{\tilde{p}}^2}}, \tag{1.11}$$

with $U_a^{\max}$ the maximum approach speed and $\Delta_{\tilde{p}}$ a tuning parameter to affect the transient leader-follower rendezvous behaviour, which results in the synchronisation error kinematics

$$\dot{\tilde{p}}^n = v_d^n - v_l^n = -U_a^{\max} \frac{\tilde{p}^n}{\sqrt{(\tilde{p}^n)^T \tilde{p}^n + \Delta_{\tilde{p}}^2}}. \tag{1.12}$$

From (1.9) and (1.11) it can be seen that as $\tilde{p}^n \to 0$ the approach speed goes to zero and the velocity of the follower approaches the leader velocity. Conversely when $\tilde{p}^n \to \infty$ the approach velocity approaches $U_a^{\max}$ and the guidance commands the maximum allowed velocity to close the gap.

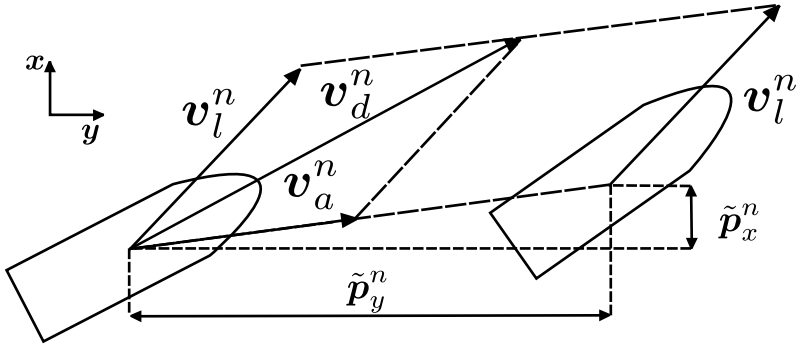

Fig. 1.1 Constant bearing guidance velocity assignments and position error.

Assumption 5. To assure that the problem is feasible we assume that the sum of the magnitude of the leader velocity, the maximum approach speed, and ocean current is smaller than the maximum feasible surge velocity of the follower U_{feas}, i.e.

$$\|v_l^n\| + U_a^{\max} + \|V_c\| \leq U_{\text{feas}} \tag{1.13}$$

for all $t > 0$. Moreover, the desired speed is required to be positive, and we therefore need to assume that

$$\|v_l^n\| - U_a^{\max} - \|V_c\| > 0 \tag{1.14}$$

for all $t > 0$.

Remark 5. Note that in order to converge to a point that is at a desired off-set w.r.t the leader p_r, the position of the leader should be included in (1.10) as $p_l^n \triangleq p_{l,\text{true}}^n + R(\psi_l)p_r$ where $R(\psi_l)$ is a rotation matrix describing the orientation of the leader. For curved paths the velocity v_l^n should then also be calculated in the off-set point to track the curvature with minimal error which requires the leader's yaw rate.

As shown in [12] the stability and convergence of the CB guidance scheme, i.e., (1.8)–(1.9) and (1.11), can be investigated using the positive definite, radially unbounded Lyapunov function candidate (LFC)

$$V = \frac{1}{2}(\tilde{p}^n)^T \tilde{p}^n. \tag{1.15}$$

Time differentiation of (1.15) along the trajectories of $\tilde{p}^n$ gives

$$\dot{V} = (\tilde{p}^n)^T (v_d^n - v_l^n) = -\kappa \frac{(\tilde{p}^n)^T \tilde{p}^n}{\|\tilde{p}^n\|} \tag{1.16a}$$

$$= -U_{a,\max} \frac{(\tilde{p}^n)^T \tilde{p}^n}{\sqrt{(\tilde{p}^n)^T \tilde{p}^n + \Delta_{\tilde{p}}^2}} < 0, \quad \forall \tilde{p}^n \neq 0 \tag{1.16b}$$

with $v_d^n - v_l^n = v_a^n$ by definition. Hence, the origin $\tilde{p}^n = 0$ is uniformly globally asymptotically stable (UGAS), which is the result given in [12].

Note however that by defining

$$\phi^*(t, \tilde{p}^n) \triangleq \frac{U_a^{\max}}{\sqrt{(\tilde{p}^n)^T \tilde{p}^n + \Delta_{\tilde{p}}^2}} \tag{1.17}$$

which for each $r > 0$ and $|\tilde{p}^n(t)| \leq r$ gives

$$\phi^*(t, \tilde{p}^n) \leq \frac{U_a^{\max}}{\sqrt{r^2 + \Delta_{\tilde{p}}^2}} \triangleq c^*(r) \tag{1.18}$$

which substituted in (1.16) gives

$$\dot{V} \leq -2c^*(r)V(t, \tilde{p}^n) \tag{1.19}$$

for all $|\tilde{p}^n(t_0)| \leq r$ and any $r > 0$. The solutions of a linear system of the form $\dot{x} = -2c^*(r)x$ are given by

$$x(t) = e^{-2c^*(r)(t-t_0)} x(t_0) \tag{1.20}$$

so by the comparison lemma [17, Lemma 3.4] we have

$$V(t, \tilde{p}^n) \leq e^{-2c^*(r)(t-t_0)} V(t_0, \tilde{p}^n(t_0)) \tag{1.21}$$

and consequently

$$\|\tilde{p}^n(t)\| \leq \|\tilde{p}^n(t_0)\| e^{-c^*(r)(t-t_0)} \tag{1.22}$$

for all $t > t_0$, $|\tilde{p}^n(t_0)| \leq r$, and any $r > 0$. Therefore, we can conclude that (1.12) is a uniformly semi-globally exponentially stable (USGES) system according to [20, Definition 2.7], a result which has not previously been shown in [12] nor [5].

Theorem 1. *Using the constant bearing guidance scheme, i.e.* (1.8)-(1.9) *and* (1.11)*, the origin of the synchronisation error kinematics* (1.12) *is uniformly semi-globally exponentially stable (USGES).*

The desired heading ψ_d and its derivative, the desired yaw rate r_d, are calculated by extracting heading information from the inner and outer products of the desired velocity v_d^n and the actual velocity v^n [8]. This assures that v^n is aligned with v_d^n. Moreover, since it provides us with course, and equivalently heading, information it allows for compensation of the environmental disturbance. More details about constant bearing guidance can be found in [12] and the references therein.

1.2.3 The Controller

The control goals are

$$\lim_{t\to\infty} \tilde{p}^n = 0, \tag{1.23}$$

$$\lim_{t\to\infty} \tilde{v}^n \triangleq v^n - v_d^n = 0, \tag{1.24}$$

which corresponds to synchronisation with the leader, i.e., that the follower vessel follows the leader, with a constant desired relative position and the same inertial frame velocity. Note that the body frame velocity may be different due to differences in actuation topology etc. In this section, we present feedback linearising controllers using the desired velocity and heading angle from 1.2.2, in order to achieve these control goals. In the following section it will be shown that the feasibility of these goals depends on the type of motion the leader executes.

Since the follower is underactuated we can not directly control the velocity in the earth-fixed coordinates, but rather the forward velocity and yaw rate in body-fixed coordinates. Therefore, we transform the velocity error in the earth-fixed frame to an error in the body-fixed frame using the coordinate transformation

$$\begin{bmatrix} \tilde{\psi} \\ \tilde{u}_r \\ \tilde{v}_r \end{bmatrix} = \begin{bmatrix} 1 & 0 & 0 \\ 0 & \cos(\tilde{\psi}+\psi_d) & \sin(\tilde{\psi}+\psi_d) \\ 0 & -\sin(\tilde{\psi}+\psi_d) & \cos(\tilde{\psi}+\psi_d) \end{bmatrix} \begin{bmatrix} \tilde{\psi} \\ \tilde{v}^n \end{bmatrix}. \tag{1.25}$$

It is straightforward to show that the Jacobian of this transformation is given by

$$\frac{\partial T}{\partial(\tilde{\psi},\tilde{v}^n)} = \begin{bmatrix} 1 & 0 & 0 \\ -\tilde{v}_x^n \mathrm{s}(\cdot) + \tilde{v}_y^n \mathrm{c}(\cdot) & \mathrm{c}(\cdot) & \mathrm{s}(\cdot) \\ -\tilde{v}_x^n \mathrm{c}(\cdot) - \tilde{v}_y^n \mathrm{s}(\cdot) & -\mathrm{s}(\cdot) & \mathrm{c}(\cdot) \end{bmatrix} \tag{1.26}$$

with $\mathrm{s}(\cdot) = \sin(\tilde{\psi} + \psi_d)$ and $\mathrm{c}(\cdot) = \cos(\tilde{\psi} + \psi_d)$. The Jacobian (1.26) can easily be verified to be non-singular. Consequently, T is a global diffeomorphism. A physical interpretation of this is that when $\tilde{\psi}$ is driven to zero, i.e., v^n is aligned with v_d^n by the CB guidance algorithm, the relative surge velocity error can be used to control v^n to v_d^n. Note that perturbation of the underactuated sway motion will disturb this balance which will be shown in the analysis of the next section.

Remark 6. For the underactuated model considered here only $\tilde{u}_r = u_r - u_d$ can be used for control purposes, while for the fully actuated case $\tilde{v}_r = v_r - v_d$ could be used to control the sway velocity and the perturbation problem does not exist. For the underactuated case the heading controller needs to assure that v^n is aligned with v_d^n and the control action can be prescribed solely by the surge actuator, something which prevents the magnitude from being matched on curved trajectories and in the presence of accelerations.

Remark 7. Note that the coupling between the heading and velocity control is what allows for disturbance rejection. Since if a larger (or smaller) velocity is needed to compensate for the effect of the current, the heading controller will assure that the vessel is rotated such that v^n and v_d^n are aligned and hence the vessel keeps the correct course.

We will use the following feedback linearising P controller for the surge velocity:

$$\tau_u = -F_{u_r}(v_r, r) + \dot{u}_d - k_{u_r}(u_r - u_d), \tag{1.27}$$

with $k_{u_r} > 0$ a constant controller gain.

Using (1.27) we can control u_r towards u_d provided that we have the acceleration of the leader available to calculate $\dot{u}_d$, but we cannot directly control v_r. Along the lines of [8] we aim to control v_r indirectly by using a proper yaw rate controller. Following [8] we have for $\tilde{\chi} = \chi - \chi_d$:

$$\sin(\tilde{\chi}) = \frac{v_d^n \times v^n}{\|v_d^n\|\|v^n\|} = \frac{\dot{y}v_{d,x}^n - \dot{x}v_{d,y}^n}{\sqrt{\left((v_{d,x}^n)^2 + (v_{d,y}^n)^2\right)(\dot{x}^2 + \dot{y}^2)}} \tag{1.28a}$$

$$\cos(\tilde{\chi}) = \frac{(v_d^n)^T v^n}{\|v_d^n\|\|v^n\|} = \frac{\dot{x}v_{d,x}^n + \dot{y}v_{d,y}^n}{\sqrt{\left((v_{d,x}^n)^2 + (v_{d,y}^n)^2\right)(\dot{x}^2 + \dot{y}^2)}} \tag{1.28b}$$

$$\tan(\tilde{\chi}) = \frac{v_d^n \times v^n}{(v_d^n)^T v^n} = \frac{\dot{y}v_{d,x}^n - \dot{x}v_{d,y}^n}{\dot{x}v_{d,x}^n + \dot{y}v_{d,y}^n} \Rightarrow \tilde{\chi} = -\mathrm{atan2}(\dot{y}v_{d,x}^n - \dot{x}v_{d,y}^n, \dot{x}v_{d,x}^n + \dot{y}v_{d,y}^n) \tag{1.28c}$$

where $\tilde{\chi} \triangleq \psi - \psi_d + \beta - \beta_d \triangleq \tilde{\psi} + \tilde{\beta}$ with $\tilde{\beta}$ the difference in side-slip angle between different orientations. We can thus define

$$\psi_d - \tilde{\beta} = \psi - \mathrm{atan2}(\dot{y}v_{d,x}^n - \dot{x}v_{d,y}^n, \dot{x}v_{d,x}^n + \dot{y}v_{d,y}^n) \tag{1.29}$$

Note that from (1.28) we also have

$$\dot{\tilde{\chi}} = \frac{\dot{x}\ddot{y} - \dot{y}\ddot{x}}{\dot{x}^2 + \dot{y}^2} + \frac{v^n_{d,y}\dot{v}^n_{d,x} - v^n_{d,x}\dot{v}^n_{d,y}}{(v^n_{d,x})^2 + (v^n_{d,y})^2} \tag{1.30}$$

so we can write

$$r_d - \dot{\tilde{\beta}} = r - \frac{\dot{x}\ddot{y} - \dot{y}\ddot{x}}{\dot{x}^2 + \dot{y}^2} - \frac{v^n_{d,y}\dot{v}^n_{d,x} - v^n_{d,x}\dot{v}^n_{d,y}}{(v^n_{d,x})^2 + (v^n_{d,y})^2} \tag{1.31a}$$

$$\triangleq r - R_1(u_r, v_r, \dot{x}, \dot{y}, v^n_d)r - R_2(v^n_d, \dot{v}^n_d) - R_3(u_r, v_r, \dot{x}, \dot{y}, v^n_d, \dot{v}^n_d) \tag{1.31b}$$

where $v^b_{c,u} \triangleq V_x\cos(\psi) + V_y\sin(\psi)$ and $v^b_{c,v} \triangleq V_x\sin(\psi) - V_y\cos(\psi)$ are the components of the current expressed in the body frame axis and

$$\begin{aligned}
R_1(\cdot) &\triangleq \frac{u_r^2 + v_r^2 + V_x^2 + X(u_r)(u_r + v^b_{c,u}) - v_r v^b_{c,v} + u_r v^b_{c,u} - v^n_{d,x}(V_x - v_r\sin(\psi))}{u_r^2 + v_r^2 + 2(u_r v^b_{c,x} + v_r v^b_{c,y}) + V_x^2 + V_y^2} \\
&\quad + \frac{-(v^n_{d,y}(v_r - v^b_{c,v}) - v^n_{d,x}v^b_{c,u})\cos(\psi) + \cos^2(\psi)(V_y^2 - V_x^2)}{u_r^2 + v_r^2 + 2(u_r v^b_{c,x} + v_r v^b_{c,y}) + V_x^2 + V_y^2} \leq C^{\max}_{R_1} \\
R_2(\cdot) &\triangleq \frac{v^n_{d,y}\dot{v}^n_{d,x} - v^n_{d,x}\dot{v}^n_{d,y}}{(v^n_{d,x})^2 + (v^n_{d,y})^2} \\
R_3(\cdot) &\triangleq \frac{Y(u_r)v_r(u_r + v^b_{c,u}) + k_{u_r}(u_r - u_d)(v_r - v^b_{c,v})}{u_r^2 + v_r^2 + 2(u_r v^b_{c,x} + v_r v^b_{c,y}) + V_x^2 + V_y^2} \\
&\quad + \frac{\dot{v}^n_{d,x}(v^b_{c,u} - v_r)\cos(\psi) + \dot{v}^n_{d,y}(V_x - v_r\sin(\psi) - v^b_{c,u}\cos(\psi))}{u_r^2 + v_r^2 + 2(u_r v^b_{c,x} + v_r v^b_{c,y}) + V_x^2 + V_y^2} \leq C_{R_3}
\end{aligned}$$

Note that R_1 can be bounded by the constant $C^{\max}_{R_1}$ since R_1 has the same growth rate in v_r and u_r for the denominator and numerator while the ocean current components are bounded (in body frame) and constant (in inertial frame). The term R_3 can be bounded by the constant C_{R_3} since the denominator and numerator grow at the same rate with respect to v_r and u_r and the current is bounded. Note that the denominator of R_1, R_2, and R_3 are larger than zero for nonzero $\|v^n\|$ and $\|v^n_d\|$ which is verified by Assumption 5. Boundedness of R_2 will be considered later since its numerator grows linearly with v_r and its denominator does not grow with v_r.

Since the inertial frame velocities, i.e. $\dot{x}$ and $\dot{y}$, are measured V_x and V_y can be substituted in expression (1.31) using the model equations (1.3a) and (1.3b) respectively for implementation purposes. Alternatively a kinematic ocean current observer as in [1] can be used to estimate $\dot{x}$, $\dot{y}$, V_x, and V_y based on measurements of the positions and relative velocities. Hence, all the variables in (1.31) are known and can thus be substituted in the yaw rate controller. A further derivative of (1.31) can be taken to obtain $\ddot{\psi}_d - \ddot{\tilde{\beta}}$ as an acceleration feedforward. Note that this will also require knowledge of the jerk of the leader motion since it contains $\dot{R}_2(v^n_d, \dot{v}^n_d)$ and $\dot{R}_3(u_r, v_r, \dot{x}, \dot{y}, v^n_d, \dot{v}^n_d)$.

To control the yaw rate we use the following controller:

$$\begin{aligned}\tau_r &= -F_r(u_r,v_r,r)+\frac{1}{R_1(u_r,v_r,\dot{x},\dot{y},v_d^n)}\Big(-\dot{R}_1(u_r,v_r,\dot{x},\dot{y},v_d^n)r-\dot{R}_2(v_d^n,\dot{v}_d^n)\\ &\quad -\dot{R}_3(u_r,v_r,\dot{x},\dot{y},v_d^n,\dot{v}_d^n)-k_\psi(\psi-\psi_d+\tilde{\beta})-k_r(\dot{\psi}-\dot{\psi}_d+\dot{\tilde{\beta}})\Big) \qquad (1.32a)\\ &= -F_r(u_r,v_r,r)+\frac{1}{R_1(u_r,v_r,\dot{x},\dot{y},v_d^n)}\Big(-\dot{R}_1(u_r,v_r,\dot{x},\dot{y},v_d^n)r-\dot{R}_2(v_d^n,\dot{v}_d^n)\\ &\quad -\dot{R}_3(u_r,v_r,\dot{x},\dot{y},v_d^n,\dot{v}_d^n)-k_\psi\tilde{\chi}-k_r\dot{\tilde{\chi}}\Big) \qquad (1.32b)\end{aligned}$$

with $k_\psi > 0$ and $k_r > 0$ constant controller gains. This control action is well defined if $R_1(u_r,v_r,\dot{x},\dot{y},v_d^n)$ satisfies certain conditions, which is something discussed in the following when considering the boundedness of r. We introduce the vector $\xi \triangleq [\tilde{u}_r,\tilde{\chi},\dot{\tilde{\chi}}]^T$, with the tracking errors $\tilde{u}_r \triangleq u_r - u_d$, $\tilde{\chi} \triangleq \tilde{\psi}+\tilde{\beta}$, and $\dot{\tilde{\chi}} \triangleq \dot{\tilde{\psi}}-\dot{\tilde{\beta}}$. The dynamics of ξ can be found by applying the controllers (1.27) and (1.32) to the dynamical system (1.3) resulting in:

$$\dot{\xi} = \begin{bmatrix}-k_{u_r} & 0 & 0\\ 0 & 0 & 1\\ 0 & -k_\psi & -k_r\end{bmatrix}\xi \triangleq \Sigma\xi. \qquad (1.33)$$

The system (1.33) is linear and time-invariant and k_{u_r}, k_ψ, and k_r are strictly positive. Consequently, Σ is Hurwitz and the origin of (1.33) is uniformly globally exponentially stable (UGES) and hence the controllers guarantee exponential tracking of the desired surge velocity and course.

Note that through the assignment of (1.32) we use the heading controller to perform course control, i.e. we force the direction of v_d^n and v^n to be equal. To investigate how the course controller affects r we start by rewriting (1.31) to obtain

$$r = \frac{1}{R_1(u_r,v_r,\dot{x},\dot{y},v_d^n)}\left(\dot{\tilde{\chi}}-R_2(v_d^n,\dot{v}_d^n)-R_3(u_r,v_r,\dot{x},\dot{y},v_d^n,\dot{v}_d^n)\right) \qquad (1.34)$$

This function is well defined if the numerator of R_1 given in (1.31) is larger than zero. This condition is satisfied if u_d is sufficiently large at all time and if u_r starts sufficiently close to u_d The term $\dot{\tilde{\chi}}/R_1$ will be bounded since $\dot{\tilde{\chi}}$ is bounded and R_1 is bounded by constant C_{R_1} as shown earlier. The same holds for the term R_3/R_1. The term R_2/R_1 however grows linearly in v_r since $\dot{v}_{d,x}^n$ and $\dot{v}_{d,y}^n$ depend linearly on v_r since the derivative of the approach speed v_a^n depends on $\dot{x}$ and $\dot{y}$. When (1.34) is substituted in (1.3e) the linear growth will assure that there is no finite escape time for v_r but some conditions have to be satisfied to show boundedness. Summarizing the above we have that the course controller results in a well defined yaw rate if the following condition is satisfied.

Condition 1. If the numerator of R_1 is strictly larger than zero, then the yaw rate equation (1.34) is well defined and bounded. In particular, besides being upper-bounded there also exists a lower bound for R_1 such that $0 < C_{R_1}^{\min} \leq R_1(u_r,v_r,\dot{x},\dot{y})$.

Remark 8. Condition 1 is satisfied for a sufficiently large desired surge velocity u_d if u_r starts in a neighbourhood of u_d. Further analysis has to be performed to find the precise physical meaning of the bound, but it appears to be that inertial frame velocity vector has to have a positive magnitude for all time. This can be satisfied by keeping the surge velocity u_r sufficiently large to be able to dominate the effects of the ocean current and the sway velocity v_r. In particular, if the inertial frame velocity vector would have a zero crossing, the rotation would change instantaneously and when the magnitude of the inertial frame velocity vector is zero then the desired rotation is undefined.

Remark 9. Note that Condition 1 is a condition that plays a role in the initial behaviour when the difference between the initial orientation of the follower and the leader is large, e.g. if they point in opposite directions. In this case u_d obtained from (1.25) needs to be saturated to a lower bound such that it stays positive and well defined. As soon as the follower is oriented in the same direction as the leader Condition 1 is easily satisfied for physically sensible motions of the leader and u_d can simply be obtained from (1.25).

The term R_2 can be interpreted as dependent on the desired curvature of the motion. In particular it can be rewritten as $R_2 = \|v_d^n\|\kappa$ where κ denotes the curvature of the desired trajectory. This term grows linearly with the inertial frame velocities of the follower since it depends on $\dot{v}_a^n$

$$R_2(v_d^n, \dot{v}_d^n) = \frac{v_{d,y}^n \dot{v}_{d,x}^n - v_{d,x}^n \dot{v}_{d,y}^n}{(v_{d,x}^n)^2 + (v_{d,y}^n)^2} = \frac{v_{d,y}^n \dot{v}_{l,x}^n - v_{d,x}^n \dot{v}_{l,y}^n}{(v_{d,x}^n)^2 + (v_{d,y}^n)^2} + \frac{v_{d,y}^n \dot{v}_{a,x}^n - v_{d,x}^n \dot{v}_{a,y}^n}{(v_{d,x}^n)^2 + (v_{d,y}^n)^2} \tag{1.35}$$

which using the transformation (1.25) can be bounded by

$$\begin{aligned} R_2 &\leq \frac{U_a^{\max}}{(v_{d,x}^n)^2 + (v_{d,y}^n)^2} \left(\frac{v_{d,y}^n + v_{d,x}^n}{\sqrt{\tilde{x}^2 + \tilde{y}^2 + \Delta_{\tilde{p}}^2}} + \frac{v_{d,y}^n(\tilde{x}^2 + \tilde{x}\tilde{y}) + v_{d,x}^n(\tilde{y}^2 + \tilde{x}\tilde{y})}{(\tilde{x}^2 + \tilde{y}^2 + \Delta_{\tilde{p}}^2)^{3/2}} \right) \tilde{v}_r + C_{R_2} \\ &\triangleq R_2' \tilde{v}_r + C_{R_2} \end{aligned} \tag{1.36}$$

where C_{R_2} is some constant which magnitude will depend on the leader's velocity and acceleration. Note that the term R_2' is uniformly bounded for desired velocities greater than zero and that it decreases as the positional error grows. Moreover, it contains two parameters that can be tuned, i.e. the maximum approach speed $U_{a,\max}$ and the interaction tuning parameter $\Delta_{\tilde{p}}$. Hence, these tuning parameters can be used to influence the interaction behaviour between r and v_r.

1.3 Closed Loop Analysis

In this section the closed-loop system, i.e. the fully actuated closed-loop dynamics, the underactuated sway dynamics, and the synchronisation error kinematics, are

investigated. In particular, the closed-loop path-following error kinematics and dynamics for (1.2) with the proposed leader-follower synchronisation scheme is given by:

$$\dot{\tilde{p}}^n = -\frac{U_a^{\max}\tilde{p}^n}{\sqrt{(\tilde{p}^n)^T\tilde{p}^n+\Delta_{\tilde{p}}^2}} + \begin{bmatrix}\tilde{u}_r\cos(\tilde{\chi}-\tilde{\beta}+\psi_d)-\tilde{v}_r\sin(\tilde{\chi}-\tilde{\beta}+\psi_d)\\ \tilde{u}_r\sin(\tilde{\chi}-\tilde{\beta}+\psi_d)+\tilde{v}_r\cos(\tilde{\chi}-\tilde{\beta}+\psi_d)\end{bmatrix} \tag{1.37a}$$

$$\dot{\tilde{v}}_r = Y(u_r)\tilde{v}_r + X(u_r)r - \dot{v}_d - Y(u_r)v_d \tag{1.37b}$$

$$\dot{\xi} = \Sigma\xi \tag{1.37c}$$

where v_d and $\dot{v}_d$ can be verified to be given by:

$$v_d = (V_x - v_{d,x}^n)\sin(\psi) - (V_y - v_{d,y}^n)\cos(\psi) \tag{1.38}$$

$$\begin{aligned}\dot{v}_d &= -\dot{v}_{d,x}^n\sin(\psi) + (V_x - v_{d,x}^n)r\cos(\psi) + \dot{v}_{d,y}^n\cos(\psi) + (V_y - v_{d,y}^n)r\sin(\psi)\\ &= -(\dot{v}_{d,x}^n + \dot{v}_{a,x}^n + (V_y - v_{d,y}^n)r)\sin(\psi) + (\dot{v}_{l,y}^n + \dot{v}_{a,y}^n + (V_x - v_{d,x}^n)r)\cos(\psi)\end{aligned} \tag{1.39}$$

with v_d bounded for a bounded leader velocity. The equation for $\dot{v}_d$ depends on $\dot{v}_{a,x}^n$, $\dot{v}_{a,y}^n$, and r which will depend on $\tilde{v}_r$. However as in (1.36) we can derive a bound for $\dot{v}_d$

$$\dot{v}_d \leq \left(\frac{\|V_c - v_d^n\|^2 R_2'}{C_{R_1}^{\min}} + \frac{U_a^{\max}}{\sqrt{\tilde{x}^2+\tilde{y}^2+\Delta_{\tilde{p}}^2}}\left(1+\frac{(\tilde{x}+\tilde{y})^2}{\tilde{x}^2+\tilde{y}^2+\Delta_{\tilde{p}}^2}\right)\right)\tilde{v}_r + C_2 \tag{1.40a}$$

$$\leq C_3\tilde{v}_r + C_2 \tag{1.40b}$$

where C_2 is a constant which will depend on the leader's maximum velocity and acceleration and on the magnitude of the ocean current. The magnitude of the constant C_3 can again be adjusted by tuning $U_a^{\max}$ and $\Delta_{\tilde{p}}$.

Please note that the terms perturbing the CB path following error system in (1.37a) compared to (1.12) arise since we here do not only consider the kinematic model, but instead take into account the (underactuated) dynamics given in (1.37b)-(1.37c). We thus take into account that the desired inertial frame velocity may not be matched since part of the error in the inertial frame velocity error is transferred to the sway direction as seen in (1.25). Note that this coupling between the underactuated dynamics and the synchronisation error kinematics was not taken into account in [5].

In order to not violate Condition 1 we analyse the system (1.37) under the following assumption.

Assumption 6. The desired relative surge velocity is saturated to a sufficiently large lower bound $u_{d,\min}$ such that Condition 1 is not violated. It is assumed that there exists such a lower bound that satisfies $u_{d,\min} < \|v_d^n\|$, i.e. that the leader velocity can be matched without violating Condition 1.

Since $u_r = u_d$ is a stable equilibrium point the surge velocity dynamics, for any $\delta > 0$ there exists a positively invariant neighbourhood of the equilibrium point such that all solutions originating in this neighbourhood satisfy $|u_r - u_d| < \delta$. Therefore in the remainder we only consider solutions starting in the neighbourhood of $u_r = u_d$ such that Condition 1 is not violated and there are no finite escape times.

Since substituting (1.34) in (1.37b) shows that there is no finite escape time for v_r and the tracking dynamics (1.37c) are UGES, it suffices to investigate local boundedness of v_r near the set where $u_r - u_d \leq \delta$ such that r is well defined. Therefore we consider the system

$$\dot{\tilde{v}}_r = Y(u_r)\tilde{v}_r + X(u_r)r - \dot{v}_d - Y(u_r)v_d \tag{1.41}$$

We substitute (1.34) and we obtain

$$\begin{aligned}\dot{\tilde{v}}_r = {} & Y(u_r)\tilde{v}_r + \frac{X(u_r)}{R_1(u_r, v_r, \dot{x}, \dot{y}, v_d^n)}\left(\dot{\tilde{\chi}} - R_2(v_d^n, \dot{v}_d^n) - R_3(u_r, v_r, \dot{x}, \dot{y}, v_d^n, \dot{v}_d^n)\right) \\ & - \dot{v}_d - Y(u_r)v_d\end{aligned} \tag{1.42}$$

Using the following Lyapunov function we show boundedness for all solutions starting in the neighbourhood of $u_r = u_d$ by considering the Lyapunov function

$$V(\tilde{v}_r) = \frac{1}{2}\tilde{v}_r^2 \tag{1.43}$$

The derivative of (1.43) along the solutions of (1.41) is given by

$$\begin{aligned}\dot{V}(\tilde{v}_r) = {} & Y(u_r)\tilde{v}_r^2 + \frac{X(u_r)\left(\dot{\tilde{\chi}} - R_2(v_d^n, \dot{v}_d^n) - R_3(u_r, v_r, \dot{x}, \dot{y}, v_d^n, \dot{v}_d^n)\right)}{R_1(u_r, v_r, \dot{x}, \dot{y}, v_d^n)}\tilde{v}_r && \text{(1.44a)} \\ & + \left(\dot{v}_d - Y(u_r)v_d\right)\tilde{v}_r \\ \leq {} & -\left(|Y^{\min}| - \frac{|X^{\max}|R_2'}{C_{R_1}^{\min}} - C_3\right)\tilde{v}_r^2 + \frac{|X^{\max}|\left(|\dot{\tilde{\chi}}| + C_{R_2} + C_{R_3}\right)}{C_{R_1}^{\min}}\tilde{v}_r && \text{(1.44b)} \\ & + (C_2 + |Y^{\max}|v_d)\tilde{v}_r\end{aligned}$$

where $Y^{\min}$, $Y^{\max}$, and $X^{\max}$ are the minimum and maximum values over the interval of velocities considered and will exist for sufficiently small δ. From which we can conclude boundedness if

$$\frac{|Y^{\min}|}{|X^{\max}|} > \frac{|R_2'|}{C_{R_1}^{\min}} + \frac{C_3}{|X^{\max}|} \tag{1.45}$$

which is a bound that depends on the leader motion, the environmental disturbance, and parameters $U_a^{\max}$ and $\Delta_{\tilde{p}}$. From (1.36) and (1.40) we can see that the term R_2' can be tuned using the parameters $U_a^{\max}$ and $\Delta_{\tilde{p}}$. In particular, if we increase $\Delta_{\tilde{p}}$, i.e. choose a smoother leader-follower rendez-vous behaviour, then the terms R_2' and C_3 will be reduced. Hence, condition (1.45) can be guaranteed to hold by appropri-

ate tuning of the constant bearing guidance algorithm and all solutions of (1.37b) originating in a neighbourhood of $u_r = u_d$ are uniformly bounded.

Remark 10. Note that increasing $\Delta_{\tilde{p}}$ has an effect on the dissipating term in (1.37a). In particular, it lowers the 'gain' of the synchronisation around the origin, i.e. the turning manoeuvre required will be less severe which has a positive effect on (1.45), but the synchronisation error increases since the follower takes a smoother trajectory.

We can now investigate the interconnection between (1.37a) and (1.37b). In particular, we show that the synchronisation error kinematics are integral input-to-state stable with respect to the output of (1.37b) and (1.37c). If we lump the perturbations into a new input $\nu(t) \triangleq [\nu_1(t), \nu_2(t)]^T$ we can rewrite (1.37a) as

$$\dot{\tilde{p}}^n = -\frac{U_a^{\max}}{\sqrt{(\tilde{p}^n)^T \tilde{p}^n + \Delta_{\tilde{p}}^2}} \tilde{p}^n + \nu(t) \tag{1.46}$$

If we consider the Lyapunov function

$$V(\tilde{p}^n) = \frac{(\tilde{p}^n)^T \tilde{p}^n}{\sqrt{(\tilde{p}^n)^T \tilde{p}^n + \Delta^2}} \tag{1.47}$$

we obtain

$$\dot{V}(\tilde{p}^n) = \frac{2(\tilde{p}^n)^T \dot{\tilde{p}}^n}{\sqrt{(\tilde{p}^n)^T \tilde{p}^n + \Delta_{\tilde{p}}^2}} - \frac{\left((\tilde{p}^n)^T \dot{\tilde{p}}^n\right)\left((\tilde{p}^n)^T \tilde{p}^n\right)}{2\left((\tilde{p}^n)^T \tilde{p}^n + \Delta_{\tilde{p}}^2\right)^{3/2}} \tag{1.48a}$$

$$\leq -\frac{2U_a^{\max}(\tilde{p}^n)^T \tilde{p}^n}{(\tilde{p}^n)^T \tilde{p}^n + \Delta_{\tilde{p}}^2} - \frac{U_a^{\max}\left((\tilde{p}^n)^T \tilde{p}^n\right)}{\left((\tilde{p}^n)^T \tilde{p}^n + \Delta_{\tilde{p}}^2\right)^2} + \frac{3}{2}\|\nu(t)\| \tag{1.48b}$$

$$\leq -\frac{2U_a^{\max}(\tilde{p}^n)^T \tilde{p}^n}{(\tilde{p}^n)^T \tilde{p}^n + \Delta_{\tilde{p}}^2} - \frac{U_a^{\max}\left((\tilde{p}^n)^T \tilde{p}^n\right)}{\left((\tilde{p}^n)^T \tilde{p}^n + \Delta_{\tilde{p}}^2\right)^2} + \frac{3\sqrt{2}}{2}\|[\tilde{u}_r, \tilde{v}_r]^T\| \tag{1.48c}$$

The first two terms are clearly negative definite and the third term is a class $\mathscr{K}$ function of the input. Consequently, (1.47) is an iISS Lyapunov function for (1.37a) [3] and the system (1.37) is iISS with respect to $\tilde{u}_r$ and $\tilde{v}_r$. The results of this section can be summarised in the following theorem.

Theorem 2. *Consider the system* (1.37)*. Under Assumptions 1-6 all the solutions of* (1.37) *starting in a neighbourhood of $u_r = u_d$ are bounded if the CB guidance algorithm is tuned such that it holds that*

$$\frac{|Y^{\min}|}{|X^{\max}|} > \frac{|R_2'|}{C_{R_1}^{\min}} + \frac{C_3}{|X^{\max}|} \tag{1.49}$$

Table 1.1 Simulation parameters.

Variable	Value	Unit	Variable	Value	Unit
$U_{a,\max}$	2	m/s	k_ψ	0.04	-
$\Delta_{\tilde{p}}$	500	m	k_r	0.9	-
V_x	-1.1028	m/s	k_{u_r}	0.1	-
V_y	0.8854	m/s			

for the given leader motion. Moreover, the synchronisation error kinematics (1.37a) *are integral input-to-state stable with respect to the output of* (1.37b)-(1.37c)*.*

Corollary 1. *If the leader trajectory is a straight-line with constant velocity then, under the conditions of Theorem 2, the synchronisation error converges to zero.*

Proof. In this case the course of the leader and its inertial frame velocity are constant. Therefore, as the follower synchronizes with the leader its course will converge to the leader's course. Since $\tilde{v}_r$ is not directly controllable the only stable configuration the follower can be regulated to, to keep a constant course, will be when $r \to 0$ and $v_r \to 0$. Consequently, both $\tilde{v}_r$ and $\tilde{u}_r$ go to zero and we arrive at the unperturbed version of (1.37a), i.e. (1.12), which has a USGES equilibrium according to Theorem 1.

1.4 Simulations

In this section two scenarios are used as case studies to validate the control strategy

1. the leader moves along a straight-line path that is at an angle with respect to the earth-fixed frame.
2. the leader moves along a sinusoidal path.

In both cases the follower ship is affected by a constant ocean current. The leader is represented by a point moving in the horizontal plane that is to be followed. This allows for a very straightforward implementation of the desired path and illustrates that the leader dynamics are not needed for the control strategy. Some parameters for the simulations are given in Table 1.1. This includes the parameters for the controllers and guidance law, and the magnitude of the ocean current. The follower vessel in the simulation is described by the ship model from [13].

1.4.1 Straight-line Path Following

The motion of the leader and the follower in the horizontal plane can be seen in Fig. 1.2. From Fig. 1.2 it can be seen that the follower converges to the trajectory of the leader and compensates for the current by side-slipping to maintain the desired

path. The side-slipping is a desired result of the control strategy and is necessary to remain on the straight-line path in the presence of ocean currents. In particular, since the vessel is underactuated in sway, a side-slip angle w.r.t. the path is necessary to compensate for the force pushing the vessel in the transverse direction of the path. Since the desired heading angle is calculated from the inner and outer products of the desired and actual velocity, the desired angle is the angle for which the velocity error is zero, which is the necessary side-slip angle.

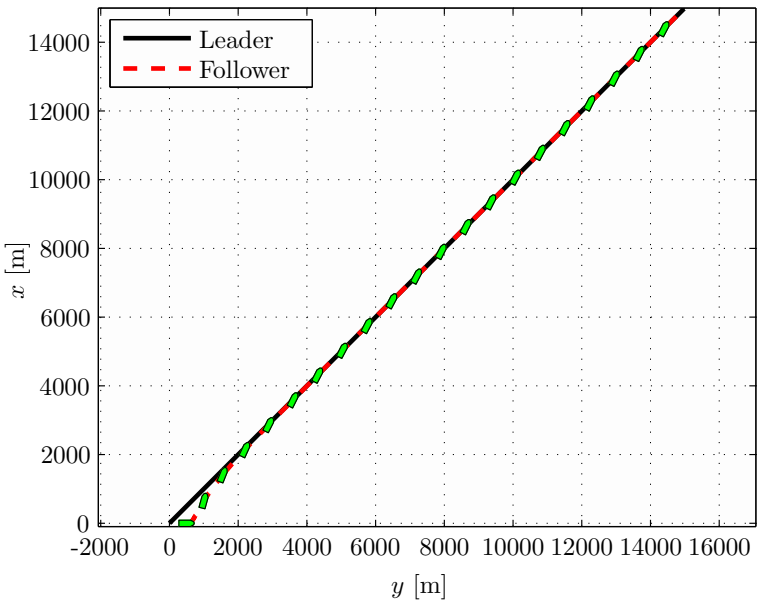

Fig. 1.2 Motion in the horizontal plane.

The synchronisation error in x and y can be seen in Fig. 1.3. Fig. 1.3 clearly shows that $\tilde{x}^n$ and $\tilde{y}^n$ converge to zero. Hence, target tracking or leader-follower synchronisation with zero synchronisation error is attained for straight-line motions with $r_d \to 0$ which is in-line with our analysis of Section 1.3.

1.4.2 Sinusoidal Path Following

In the second case study the leader generates a sinusoidal reference for the follower which demands a constantly changing desired yaw rate. Hence, the synchronisation error kinematics are perturbed.

The trajectory of the leader and the follower for tracking of a sinusoidal path can be seen in Fig. 1.4. From Fig. 1.4 it can be seen that the follower gets close to the trajectory of the leader and compensates for the current to maintain the desired

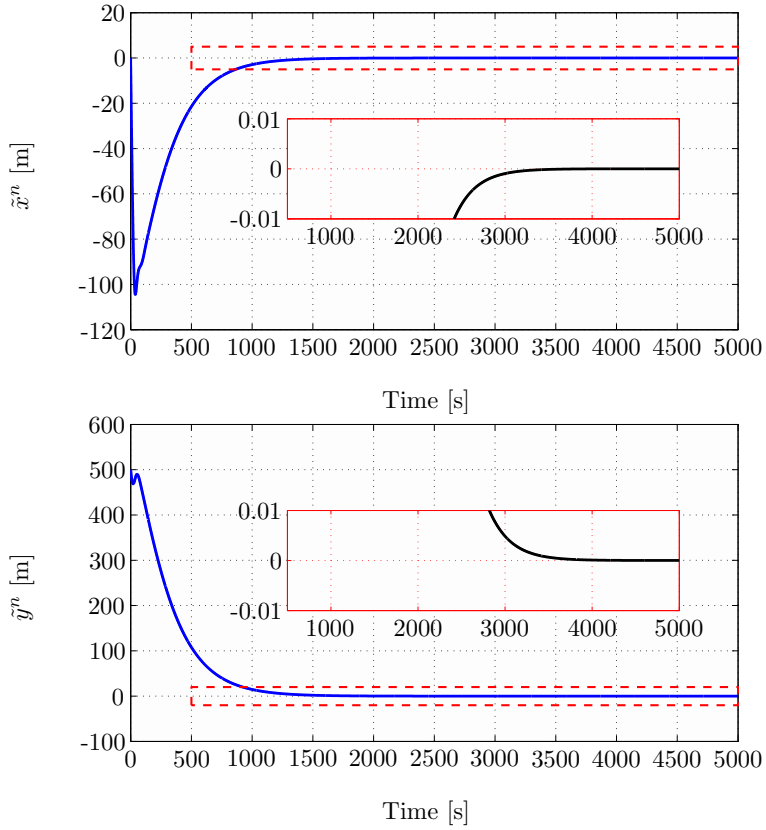

Fig. 1.3 x (top) and y (bottom) synchronisation error.

path. Fig. 1.5 shows the position synchronisation error in the x and y direction. From Fig. 1.5 it can be seen that the synchronisation error in x decreases to below an amplitude of about 1.5 meters, while the error in y direction, which is the direction transversal to the propagation of the sinusoid and most prone to drift, decreases to below 2.5 meter. Note that the error plots are asymmetric due to the vessel changing its direction with respect to the current which causes different behaviour.

The behaviour in the test-case is in-line with the analysis of Section 1.3 since we have convergence from large initial errors, the follower converges towards the trajectory of the leader. When the follower is close to the leader the follower exhibits integral input-to-state stable behaviour and stays in a neighbourhood of the leader dependent on the size of the desired yaw rate to track this motion.

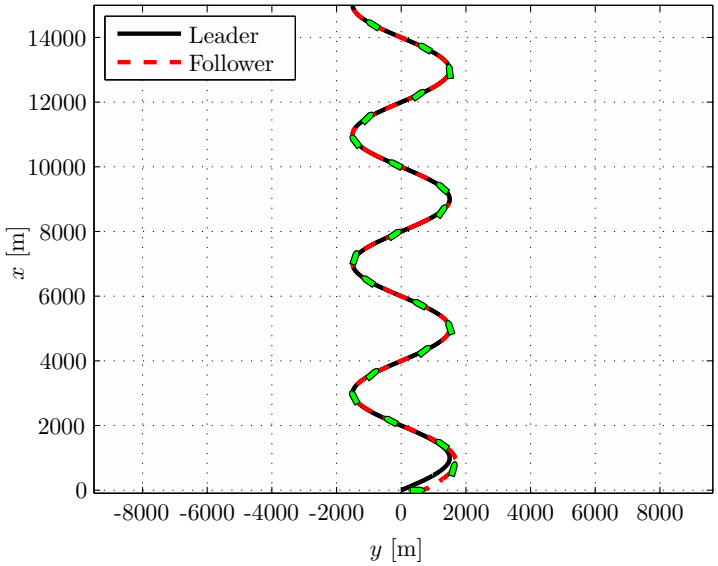

Fig. 1.4 Motion in the horizontal plane.

1.5 Conclusions

This chapter has presented and analysed a control scheme for leader-follower synchronisation for inhomogeneous multi-agent systems consisting of an underactuated follower and a leader vessel with unknown dynamics. The developed leader-follower scheme can be applied to multi-agent systems with underactuated follower agents that are subjected to environmental disturbances. The dynamics of the leader is unknown, and the leader may be fully actuated or underactuated. Position and velocity measurements of the leader are available to the follower for use in the guidance law. If the follower uses controllers with acceleration feedforward, acceleration and jerk measurements of the leader also need to be available to the follower. The leader is free to move as it wants independently of the follower(s), and can for instance be manually controlled. The follower thus has no information about the future motion of the leader. The follower uses a constant bearing guidance algorithm to track the leader. The constant bearing guidance algorithm is shown to provide USGES synchronisation error kinematics. The constant bearing guidance algorithm is then coupled to controllers designed for the underactuated follower vehicle. This results in a closed-loop system consisting of the fully actuated controlled dynamics, underactuated dynamics, and synchronisation error kinematics. The solutions of the underactuated and the fully actuated dynamics, have been shown to be bounded under certain conditions. Furthermore, the synchronisation error kinematics has been shown to be integral input-to-state stable with respect to changes in the unactuated sway velocity. Moreover, it has been shown that synchronisation can be achieved when the leader moves along a straight-line since in this case the perturbation of

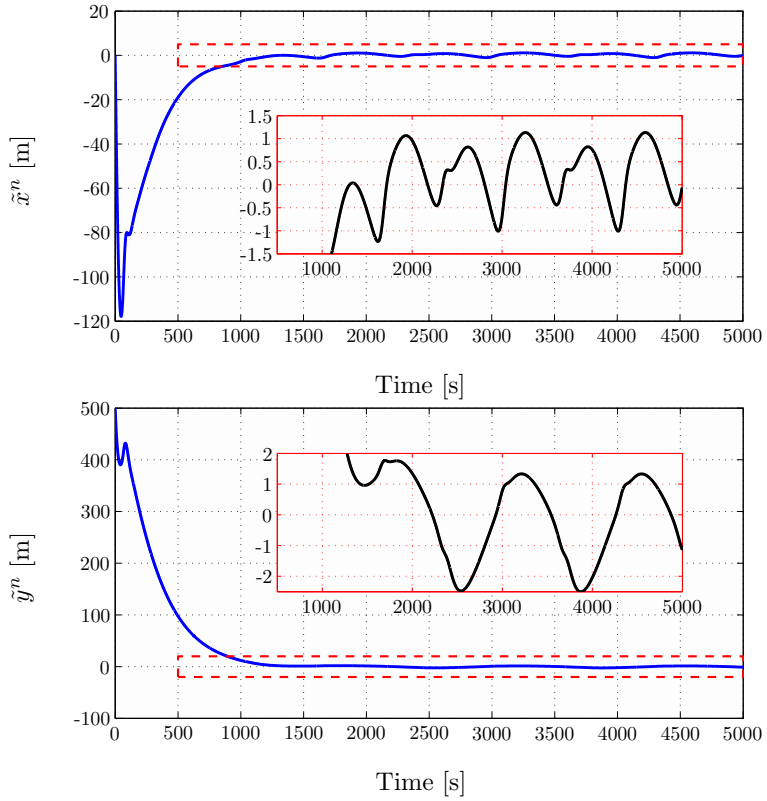

Fig. 1.5 x (top) and y (bottom) synchronisation error.

the underactuated dynamics to the synchronisation error kinematics vanishes. The validity of the control scheme has been shown in a case study.

Acknowledgements The authors would like to thank Erjen Lefeber for the valuable discussions on and inputs to the material presented in this chapter.

References

1. A. P. Aguiar and A. M. Pascoal. Dynamic positioning and way-point tracking of underactuated auvs in the presence of ocean currents. *International Journal of Control*, 80(7):1092–1108, 2007.
2. A.A. Aguirre. *Remote Control and Motion Coordination of Mobile Robots*. PhD thesis, Technische Universiteit Eindhoven, 2011.
3. D. Angeli, E. D. Sontag, and Y. Wang. A characterization of integral input-to-state stability. *IEEE Transactions on Automatic Control*, 45(6):1082–1097, 2000.

4. D.J.W. Belleter and K.Y. Pettersen. Path following for formations of underactuated marine vessels under influence of constant ocean currents. In *Proceedings of the 53th IEEE Conference on Decision and Control, Los Angeles, USA, Dec. 15-17*, pages 4521–4528, 2014.
5. D.J.W. Belleter and K.Y. Pettersen. Underactuated leader-follower synchronisation for multi-agent systems with rejection of unknown disturbances. In *American Control Conference (ACC), Chicago, USA*, pages 3094–3100, 2015.
6. M. Breivik and T.I. Fossen. Guidance laws for planar motion control. In *Proc. of the 47th IEEE Conference on Decision and Control, Cancun, Mexico*, pages 570–577, 2008.
7. M. Breivik, V.E. Hovstein, and T.I. Fossen. Ship formation control: A guided leader-follower approach. In *Proc. IFAC World Congress, Seoul, Korea*, 2008.
8. M. Breivik, V.E. Hovstein, and T.I Fossen. Straight-line target tracking for unmanned surface vehicles. *Modeling Identification and Control*, 29(4):131–149, 2008.
9. W. Caharija, K.Y. Pettersen, and J.T. Gravdahl. Path following of marine surface vessels with saturated transverse actuators. In *American Control Conference (ACC), Washington, USA*, pages 546–553, 2013.
10. J. Dasdemir and A. Loría. Robust formation-tracking control of mobile robots via one-to-one time-varying communication. *International Journal of Control*, pages 1–17, 2014.
11. J.P. Desai, J.P. Ostrowski, and V. Kumar. Modeling and control of formations of nonholonomic mobile robots. *IEEE Transactions on Robotics and Automation*, 17(6):905–908, 2001.
12. T.I. Fossen. *Handbook of Marine Craft Hydrodynamics and Motion Control*. Wiley, 2011.
13. E Fredriksen and K.Y. Pettersen. Global κ-exponential way-point manoeuvering of ships. In *Decision and Control, 2004. CDC. 43rd IEEE Conference on*, volume 5, pages 5360–5367. IEEE, 2004.
14. E. Fredriksen and K.Y. Pettersen. Global κ-exponential way-point maneuvering of ships: Theory and experiments. *Automatica*, 42(4):677–687, 2006.
15. S.H. Fu and W.M. Haddad. Nonlinear adaptive tracking of surface vessels with exogenous disturbances. *Asian Journal of Control*, 5(1):88–103, 2003.
16. W.M Haddad, S.G. Nersesov, Q. Hui, and M. Ghasemi. Flocking and rendezvous control protocols for nonlinear dynamical systems via hybrid stabilization of sets. In *IEEE Proc. 52nd Conference on Decision and Control (CDC), 2013*, pages 2151–2156. IEEE, 2013.
17. H.K. Khalil. *Nonlinear Systems*. Prentice Hall, Inc., 2002.
18. E. Kyrkjebø. *Motion Coordination of Mechanical Systems*. PhD thesis, Norwegian University of Science and Technology, 2007.
19. E. Kyrkjebø, K.Y. Pettersen, M. Wondergem, and H. Nijmeijer. Output synchronization control of ship replenishment operations: Theory and experiments. *Control Engineering Practice*, 15(6):741–755, 2007.
20. A. Loría and E. Panteley. Cascaded nonlinear time-varying systems: Analysis and design. In *Advanced topics in control systems theory*, pages 23–64. Springer, 2005.
21. H. Nijmeijer and A. Rodriguez-Angeles. *Synchronization of mechanical systems*. World Scientific, 2003.
22. Z. Peng, D. Wang, Z. Chen, X. Hu, and W. Lan. Adaptive dynamic surface control for formations of autonomous surface vehicles with uncertain dynamics. *IEEE Transactions on Control Systems Technology*, 21(2):513–520, 2013.
23. H.A. Poonawala, A.C. Satici, and M.W. Spong. Leader-follower formation control of nonholonomic wheeled mobile robots using only position measurements, istanbul, turkey. In *9th Asian Control Conference (ASCC)*, pages 1–6, June 2013.
24. R. Skejic, M. Breivik, T.I. Fossen, and O.M. Faltinsen. Modeling and control of underway replenishment operations in calm water. In *8th Manoeuvring and Control of Marine Craft, Guarujá, Brazil*, pages 78–85, 2009.